Infrared Radiation Thermometry of Guatemalan Volcanoes

R. W. BIRNIE
Department of Earth Sciences, Dartmouth College, Hanover, New Hampshire 03755 *

Abstract

A Barnes PRT-5 radiation thermometer was used to obtain apparent surface temperatures of two Guatemalan volcanoes from land-based stations from 500 to 4000 meters distant. Isotherms of apparent surface temperatures, drawn on photographs of the volcanic terrain under study, delineate areas of fumarolic activity and active domal upgrowth.

The excess radiant heat emitted from Pacaya Volcano is calculated from apparent surface temperatures corrected for atmospheric absorption of infrared radiation and for the adiabatic cooling of the atmosphere with altitude. The excess radiant heat data indicate that the lava flow extruded in June 1969 had completely solidified by December 1969. This calculation is consistent with theoretical estimates of the cooling of an extrusive lava sheet by conduction. Similar calculation of excess radiant heat emission shows the depth of the magma chamber underlying the Santiaguito Volcanic Dome to be 11 meters. This depth is consistent with field observations.

Corrections are made for surface emissivity on Pacaya Volcano and the isotherms of real surface temperature plotted. Consideration is given to the times required for the equilibration of a geothermal gradient following the upward movement of a magma.

Introduction

The Central American volcanic chain strikes northwest-southeast across Guatemala. Separate volcanic ridges strike normal to the major trend. A coastal plain up to 80 km wide runs parallel and lies to the southwest of the volcanic chain whose highest peaks

* Presently at Department of Geological Sciences, Harvard University, Cambridge, Massachusetts 02138.

attain altitudes of 4000 m. An intensely folded and metamorphosed eugeosynclinal mountain belt lies northeast of the volcanic chain. The volcanic and geologic history of the area is discussed in detail by WILLIAMS (1960) and MEYER-ABICH (1958). The geographic relationship of the two Quaternary volcanoes, Santiaguito and Pacaya, in this study is shown in Fig. 1.

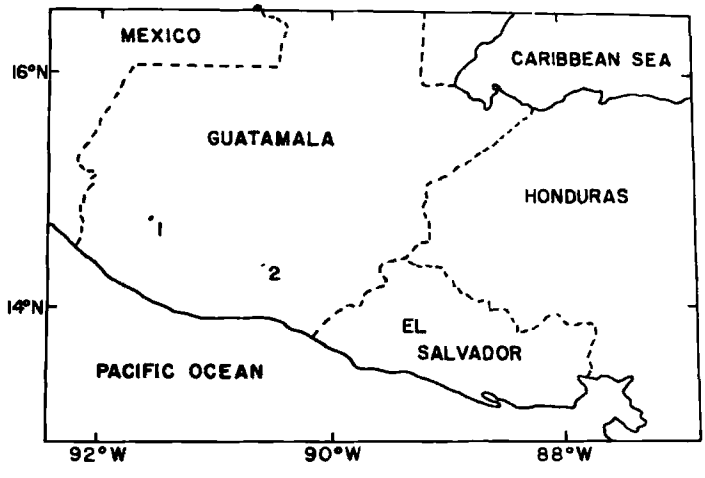

FIG. 1 - Sketch map of a portion of Central America indicating the location of Santiaguito Volcanic Dome (1) and Pacaya Volcano (2) (after MOOSER, *et. al.*, 1958, p. xi).

Santiaguito is a volcanic dome located 12 km southwest of Quezaltenango, Guatemala. The dome lies in the 1902 explosion crater on the southwest flank of Santa Mariá Volcano. The dacitic dome is made up of 14 chronologically related units, the first of which was extruded in 1922 (ROSE, 1972). The history, geology, and fumarolic activity at Santiaguito have been described by ROSE (1972 and 1970), STOIBER and ROSE (1969), and ROSE *et al.* (1970).

Pacaya Volcano is part of a volcanic complex south of Guatemala City. The volcano is located where the two bordering faults of the Guatemala City Valley graben intersect. The original cone of Pacaya is marked by a fault scrap, indicated today by hot springs around the village of San Francisco and Laguna des Calderas. The Cerro Grande Dome lies along the eastern border of the ancient caldera. Smaller and more recent domes are located at the north base of

Pacaya on the shores of Lake Amatitlán. The present summit cone of Pacaya Volcano rises 2552 m above sea level. The first recorded eruptions occurred in 1565 (MEYER-ABICH, 1958, p. 66). After 100 years of quiescence, Pacaya resumed activity in 1961 with lava flows from its south flank. In August, 1965, eruptive activity commenced in a collapse crater to the west of the summit cone and has continued to the present. The older Pacaya lavas are hornblende-pyroxene andesite rich in olivine (MEYER-ABICH, 1958, p. 66), while the more recent products are olivine basalts (ROSE, 1967). The geology of Pacaya and the surrounding area has been studied in detail by EGGERS (1972).

Previous Work

The first report on the ability to render a thermal pattern visible was made by Sir John HERSCHEL (1840), the son of Sir Frederick William Herschel, the discoverer of infrared radiation. On paper especially treated with spirit of wine, Sir John Herschel (1840, p. 53) was able to record thermal radiation emitted by the sun in the near and the intermediate infrared region. The sun's rays were refracted through a prism and the visible parts of the spectrum were marked. The thermal pattern was observed beyond the red end of the visible spectrum. The thermal pattern was produced by the differential evaporation rates of the spirit of wine on areas of the paper that received different amounts of thermal radiation.

Since this original work, technology has advanced to the point where electronic radiation thermometers have been developed to measure the intensity of radiant existance at specific wavelengths or within particular spectral bands. These instruments have been made portable for use in the field and have been adapted for use in airplanes and satellites. These radiation thermometers are capable of measuring the relatively low levels of terrestrial infrared radiation.

Airborne infrared radiation thermometers have been used to detect thermal emissions from volcanic and geothermal areas. Work during the decade from 1958-1968 has been summarized by FRIEDMAN and WILLIAMS (1968). They report that several geothermal fields and 22 volcanoes were surveyed by infrared techniques during that period. Infrared systems recorded effusive volcanic activity at Kilauea, Etna, and Surtsey (FRIEDMAN and WILLIAMS, 1968, p. 788). Thermal anomalies indicated a change in the thermal regime of Askja Volcano,

Iceland prior to its eruption in 1961 (FRIEDMAN and WILLIAMS, 1968, p. 788).

Curvilinear fault patterns associated with the Kilauea Caldera, Hawaii (FISCHER, *et al.*, 1964, p. 735), the central crater of Taal Volcano Philippines (MOXHAM and ALCARAZ, 1966, p. 830), and the summit crater of Mt. Rainier, Washington (MOXHAM, *et al.*, 1965, p. D93) have been manifested on airborne infrared imagery. Thermal features in the Cascade Range have been summarized by MOXHAM (1971). Linear and en echelon fault systems associated with rift zones have been indicated on airborne infrared imagery along the southwest rift zone of Kilauea (FISCHER, *et al.*, 1964, p. 735) and in the Icelandic rift zone (FRIEDMAN and WILLIAMS, 1968, p. 788).

Using an airborne infrared sensor, MOXHAM (1969, p. C115) reported that the most intense thermal anomalies in the Geysers area of California coincided with the region of hydrothermally altered and steaming ground with the thermal maximum occurring over active fumaroles and hot springs. Infrared thermal sensing devices have been flown over several volcanoes along the Kamchatka Peninsula in Russia. These studies have delineated fumarolic areas and fault patterns (SHILIN and KOMAROV, 1968; SHILIN, *et al.*, 1969; and SHILIN and GUSEV, 1969). Hydrothermal features have also been mapped from the air in Yellowstone National Park (MCLERRAN and MORGAN, 1964; and MILLER, 1966).

Infrared surveys have been used to determine the proportion of total heat flow from a cooling body that is emitted as radiant energy. At Alae Lava Lake, Hawaii, 10 % of the heat flow to the surface over a whole day was emitted as radiant energy (DECKER and PECK, 1967, p. D175). About 4 % of the thermal energy in a lava flow on Surtsey Volcano, Iceland exited the earth's atmosphere as radiant emission (FRIEDMAN and WILLIAMS, 1968, p. 815). The Friedman and Williams study (1968) used data obtained from an infrared sensor employing the 3.45-4.07 μ band in the Nimbus II satellite. DECKER and PECK (1967) used a land-based radiation thermometer measuring in a wavelength band greater than 3 μ from a height above the surface of one foot.

To date, two main uses for infrared thermal images of volcanic features have manifested themselves. Infrared thermal images have depicted the relative intensity of anomalous geothermal features in an area. Secondly, infrared thermal images have been able to relate thermal anomalies to structural and tectonic patterns such as faults

caused by rifting or caldron subsidence in volcanic areas. These airborne studies are primarily qualitative; and in general, they merely confirm the presence of geothermal and structural features already well known from field observations. A method of obtaining quantitative information as to magma chamber depths from land-based infrared surveys will be discussed in this paper. To the best of this author's knowledge, the study described herein is the first land-based attempt to remotely obtain an infrared thermal pattern of volcanic terrain.

Instrumentation and Procedure

The radiation thermometer used in this study is a Barnes PRT-5 Precision Radiation Thermometer, manufactured by the Barnes Engineering Company of Stamford, Connecticut. A general description of the instrument's specifications and electronics which are summarized in an instruction manual (BARNES, 1968) follows.

The instrument measures the 8-14 μ radiant exitance of any target in its two degree field of view. The two degree field of view « sees » a circle about 3 m in diameter at a distance of 100 m from the sensor. The instrument is completely portable. It operates from either a built-in battery pack or external power. The radiation thermometer has about eight hours of battery time when operating at ambiant temperatures about 25°C. The instrument can operate at ambiant temperatures between −20 and +40°C.

The instrument consists of two units, an Optical and an Electronics Unit. The Optical Unit contains an internal reference standard held at 45°C ± 1/2°C. This unit continually compares the radiant exitance of the target with that of the internal reference standard. The Electronics Unit converts this energy difference to a voltage that is metered in terms of irradiance at the radiometer (μ watts/cm²). The time constant of the radiation thermometer is 50 milliseconds at 30 cps bandwidth. A thermistor oblometer is used as the radiation detector. It measures equivalent blackbody temperatures between −42°C and +65°C ± 1/2°C. The thermistor sensing area is a 50 μ square on the back of a germanium lens. The Optical Unit is spectrally filtered to the 8-14 μ band. The radiometry units in the present study are in acccordance with those outlined by MEYER-ARENDT (1968).

This survey was land-based. Each station was chosen so as to command a view of the volcano whose thermal pattern was of interest. A Polaroid photo was then taken of the area under consideration. These photos were most often taken on the day preceeding the survey. A grid representing a 2° field of view was lain over the photo. In this way, the scene was sectioned off in 2° boxes representing the 2° field viewed by the radiation thermometer. A rifle-type sight is located on the Optical Unit of the radiation thermometer. With the aid of this sight, the Optical Unit was pointed at a particular area that could be located on the Polaroid photo and identified by the grid system. The Optical

Unit was held fixed on a tripod while the radiant exitance was read off the Electronics Unit and recorded. In this way, the radiant exitance at any point of the field could be measured and documented. The radiant exitance at each point represented radiant exitance integrated over the whole 2° field of view. The radiant exitance was converted to an equivalent blackbody temperature according to calibration tables of the Barnes Engineering Company (BARNES, 1968). The following thermal patterns are based on apparent surface temperatures. No correction is made for the emissivity of the surface material or atmospheric absorption of infrared radiation.

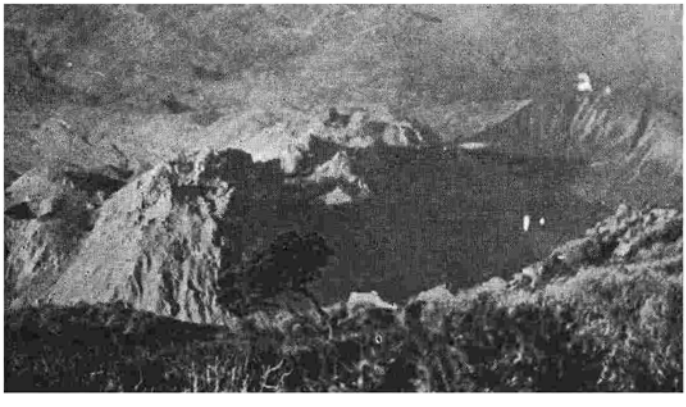

FIG. 2 - Santiaguito Volcano as seen from the summit of Santa Mariá Volcano, December 1969. The Caliente Crater and El Brujo Dome are at the far left and right of Santiaguito respectively. La Isla (1) and La Loma (2) are noted at the right of the photo.

The recordings were taken at early dawn before the sun directly shone on the volcano. In this way, the influence of differential solar heating on the surface materials was minimized. The volcanic surfaces were of constant composition, therefore, the emissivities were constant, but not unity. Therefore, any thermal anomalies are related to differential geothermal heating, not differential solar heating or differential surface emissivity.

Thermal Patterns of Santiaguito Volcanic Dome

The most continuously active area on Santiaguito is the Caliente Crater located at the eastern end of the dome and about 1500 m below the summit of the parent volcano, Santa Mariá (Fig. 2 and 3). This crater has been the site of intense fumarolic and explosive activity. Individual fumaroles have had temperatures of 843°C (STOIBER and ROSE, 1969, p. 484-485), indicating the proximity of the magma

to the surface. The thermal pattern of the Caliente Crater area was mapped on the early morning of 20 December 1969 (Fig. 4) from a station on the summit of Santa Mariá.

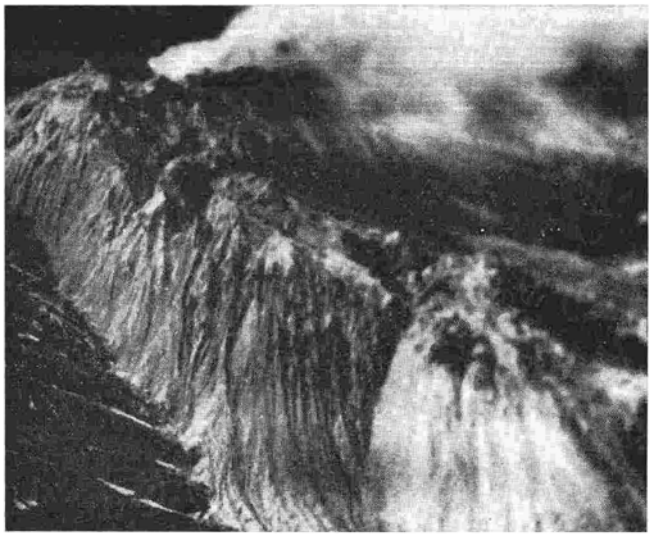

FIG. 3 - Oblique airphoto of Santiaguito. The El Brujo Dome is at the lower right and the Caliente Crater is seen steaming about 1.3 km to the east. The relief of Santiaguito is 450 m. *Photo by Instituto Geografico Nacional of Guatemala, August 1967.*

The hottest part of the dome is congruent with the recent explosive vent at H-8 (Fig. 4). Apparent surface temperatures are seen to increase up slope toward the explosive vent. The irregular thermal pattern across grid row 10 is due to varying atmospheric conditions while this row was being mapped. Small clouds sporadically occupied a portion of the field of view of the radiation thermometer and caused irregular, lower apparent surface temperatures.

The El Mitad Dome on the right side of Fig. 4 shows uniform apparent surface temperatures of about 9° and 10°C. Most of the area to the right of grid column K is bare dome rock, while the area to the left of grid column K is blanketed with a thin veneer of fine ash erupted from the Caliente vent.

Santiaguito (Fig. 5) extends from left to right about 1400 m with a maximum relief of about 350 m. Figure 5 includes from left to right the El Mitad Dome, the El Monje Dome, and the El Brujo

Dome as seen from La Buena Vista located on the west flank of Santa Mariá Volcano. These thermal patterns were mapped on the early mornings of 22 December 1969 and 30 March 1970.

It is apparent in Fig. 5 that Santiaguito shows increasing apparent surface temperatures with altitude. This is inconsistent with the adiabatic cooling of the atmosphere with altitude and is a reversal

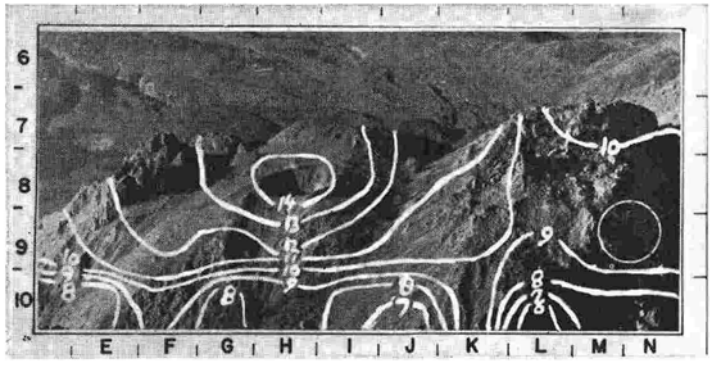

FIG. 4 - Thermal pattern of Caliente Dome, Santiaguito Volcano, looking down to the southwest from summit of Santa Mariá Volcano, 20 December 1969. Caliente explosive vent is seen at 8-H. Contours indicate apparent surface temperatures in °C. Grids enclose surfaces 70 ± 20 m on a side. Circle to right represents 2° field of view of radiation thermometer.

of the patterns observed at Pacaya Volcano which are described below. The top of Santiaguito is bare rock that has been gradually extruded upward with the growth of the individual domal units. Material is continually breaking off the upper slopes of Santiaguito and rolling down the lower slopes forming a thick talus blanket. This talus blanket has an insulating effect that hinders the conduction of heat out from the magma chamber to the surface. The upper levels of Santiaguito are devoid of this insulating talus blanket and, therefore, have higher apparent surface temperatures.

The apparent surface temperatures on the early morning of 30 March 1970 (Fig. 5 bottom) were on the average 2°C warmer than those of the early morning of 22 December 1969 (Fig. 5 top). The average minimum air temperatures for the region around Santiaguito are also 2°C warmer at the end of March than in December (VASSEAU, 1967).

Figure 5 shows anomalously hot apparent surface temperatures in grids I-8 and 0-9. The Sapper and Bonis Fumaroles, respectively,

are continuously emitting hot steam vapors in these regions (STOIBER and ROSE, 1969, p. 497). The hot steam radiates heat to the region around it and produces a broad hot thermal anomaly. The active El Brujo Dome is located at the far right of Fig. 5 and a sharp thermal gradient is seen to increase up and to the right across this dome.

Figure 5 demonstrates the ability of remotely obtained infrared radiation thermal data to delineate areas of active domal upgrowth

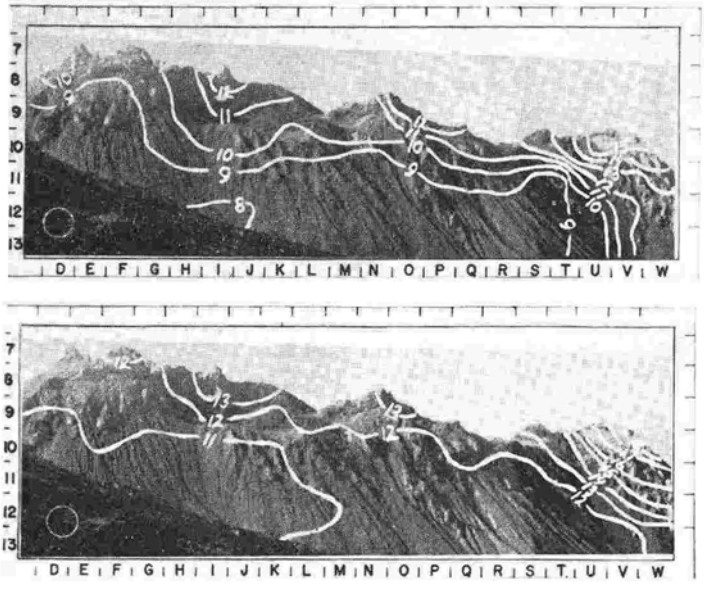

FIG. 5 - Thermal pattern of Santiaguito Volcano looking southwest from La Buena Vista, 22 December 1969 (top) and 30 March 1970 (bottom). Contours indicate apparent surface temperatures in °C. Grids enclose surfaces 80 ± 30 m on a side. Circle at lower left represents 2° field of view of radiation thermometer.

insofar as this growth is manifested by abnormally high apparent surface temperatures. Active fumarolic areas are also located by their local high temperature anomalies.

The El Brujo Dome was shown to be an active thermal area in Fig. 5. The north face of this dome was thermally mapped in greater detail from a station on La Isla (Fig. 2) on the early mornings of 21 December 1969 and 27 March 1970 (Fig. 6). About 180 m of relief are present in Fig. 6. It is from this vantage point that STOIBER and ROSE (1969, p. 489) trace the growth of the dome between February 1967 and February 1968.

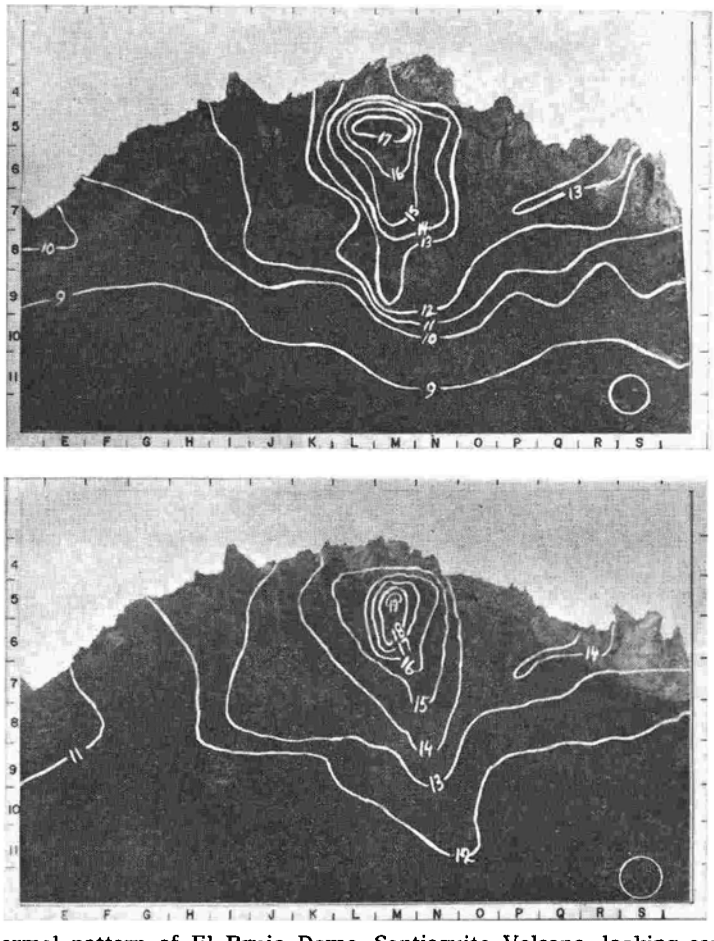

FIG. 6 - Thermal pattern of El Brujo Dome, Santiaguito Volcano, looking south from La Isla, 21 December 1969 (top) and 27 March 1970 (bottom). Contours indicate apparent surface temperatures in °C. Grids enclose surfaces 20 ± 6 m across slope and 30 ± 10 m up slope. Circle at lower right repsentents 2° field of view of radiation thermometer.

It is clear from an inspection of these patterns (Fig. 6) that the center of the geothermal activity is at grid square M-5. The hottest area in the December 1969 pattern (Fig. 6 top) is located directly below a fresh Pelean spine that has been extruded upward. The upward growth of the north face of El Brujo radiates from the hot spot at M-5. By March 1970 (Fig. 6 bottom), the sharp spine had broken off and the skyline profile was smoother. The skyline from the sharp spine in I-4 to the left showed no change between December

1969 and March 1970. Close inspection of the talus slope below this area shows that many of the rocks that were laying loose on the slope in December 1969 were still present in March 1970. The right skyline underwent considerable change between December 1969 and March 1970.

The center of the thermal activity in Fig. 6 closely corresponds to the vents of a series of small nuées ardentes that issued from El Brujo between July and November 1967 (STOIBER and ROSE, 1969, p. 493 and figs. 13 and 14).

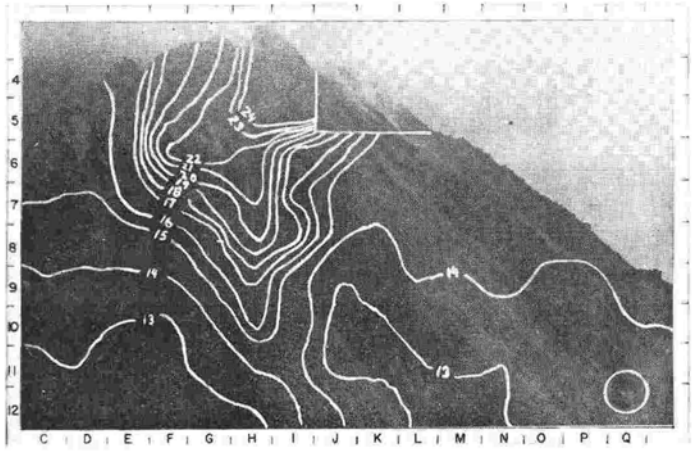

FIG. 7 - Thermal pattern of El Brujo Dome, Santiaguito Volcano, looking southeast from La Loma, 29 March 1970. Contours indicate apparent surface temperatures in °C. Grids enclose surfaces 38 ± 9 m across slope and 62 ± 14 m up slope. Circle at lower right represents 2° field of view of radiation thermometer.

The 10°C and 12°C apparent temperature isotherms on the December 1969 and March 1970 profiles, respectively, approximate the contact between the hard lava above and the loose talus below. From these isotherms, the apparent surface temperatures increase sharply upward and decrease gradually downward. As is manifested in the overall thermal patterns of Santiaguito from Buena Vista (Fig. 5), the apparent surface temperatures in March 1970 are about 2°C warmer than those of December 1969. This is consistent with the average seasonal air temperature trends in the region (VASSEAU, 1967).

The northwest face of El Brujo Dome was thermally mapped on the early morning of 29 March 1970 (Fig. 7). This thermal pattern

was obtained from La Loma located on the ridge above La Isla (Fig. 2). These are about 350 m of relief on this northwest face of El Brujo in Fig. 7. The hard rock outcropping at G-6 in Fig. 7 is equivalent to the rock spines seen on the skyline at R-6 and S-6 of Fig. 6.

The isotherms of apparent surface temperatures on Fig. 7 indicate the center of thermal activity is in the upper-right portion of the dome. Field observations noted a steaming lava outcrop in this area that can be seen in Fig. 7 at K-5. This area was not thermally mapped, because on the early morning of 29 March 1970, this area was covered by clouds. The clouds were induced by the large quantities of steam being emitted from this active area. This hot thermal anomaly appears to be the vent from which a series of viscous lava flows were extruded between January 1959 and early 1963 (STOIBER and ROSE, 1969, p. 490-491).

Hot rocks are continually breaking off the upper slopes of El Brujo, especially in the regions of G-5 and I-4. These hot rocks roll down the talus slope out of the area covered by Fig. 7 at I-12, J-12, and K-12. The active talus area is marked by distinctly lighter colored surface material in Fig. 7. Apparent surface temperatures are abnormally hot in this active area due to the influence of the hot rocks rolling down slope.

Thermal Patterns of Pacaya Volcano

The northwest flank of Pacaya Volcano was thermally mapped from the northwest rim of an old explosive vent known as Cerro Chino (Fig. 8). This station affords an excellent view of the vent of present activity on Pacaya as well as the deposit left by a lava flow in June 1969 (Fig. 9). Thermal patterns on the northwest flank of Pacaya Volcano were mapped on three occasions: 23 December 1969, 30 December 1969, and 31 March 1970 (Fig. 10). The portion of the volcano covered in Fig. 10 represents about 300 m of relief. Eruptive activity has been going on since August 1965 (ROSE, 1965, p. 1) and is centered in the collapse feature on the west flank of the volcano seen in Fig. 8. The cone that has been built up by pyroclastic eruptions is seen in profile at S-12 of Fig. 10. Hot pyroclastics from this cone blanket much of the west flank of the volcano. The area covered by these pyroclastics is sectioned off in the figures showing the thermal

patterns. Irregular temperatures that were often greater than the maximum range of the radiation thermometer (65°C) were measured in this area. Since temperature patterns in this area are the result of loose material on the surface and not an underlying geothermal anomaly, this area is deleted from consideration. Eruptive activity

FIG. 8 - Vertical airphoto of Pacaya Volcano, Guatemala. North is at top left. Cerro Chino station is at upper left (1). Finca El Chupadero station is off photo at the bottom to the left of the dark lava flow. The photo was taken prior to the present eruptive activity. The depression and vegetation on the west flank of the volcano are no longer present. Scale approximately 1/12,500. *Photo taken by Instituto Geografico Nacional of Guatemala, 3 August 1963.*

was much greater on 31 March 1970 than the days of the two previous thermal observations. Hot pyroclastics were falling over a greater area. For this reason, a greater region is deleted from this thermal pattern.

The general features of the three thermal patterns are the same. A linear-shaped hot thermal anomaly points up slope towards the eruptive vent. The difference in apparent surface temperature between the hottest area and coolest area on each of the thermal patterns ranges from 7°C on 30 December 1969 to 9°C on 31 March 1970. The

apparent surface temperatures cool to the left and right of the thermal anomaly and up slope. The hot thermal anomaly stretches farther to the left and the cooling gradient is much sharper on 31 March 1970 than on the other two days. This is due to the presence of a few hot pyroclastics covering the lower portions of grid columns 4-13. Field observations on the morning of 31 March 1970 indicated that occa-

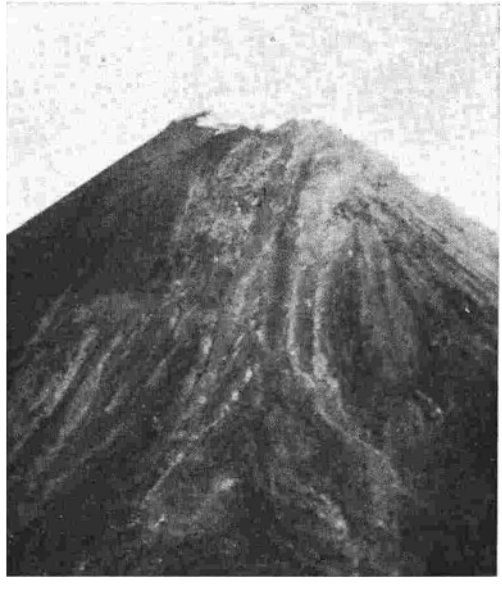

FIG. 9 - Photo of Pacaya Volcano looking southeast from Cerro Chino. The two tongues o fthe June 1969 lava flows are seen as lighter colored material on the central part of the volcano. *Photo by Albert A. Eggers, July 1969.*

sional pyroclastics from the explosive vent were rolling the northwest side of the volcano and coming to rest in the lower portions of the area included in this thermal pattern. Due to the impossible task of precisely locating the areas in this thermal pattern where hot pyroclastics were lying and quantitatively determining their contribution to the apparent surface temperatures, no inference as to underlying geothermal features will be made on the basis of this thermal pattern.

Reference to Fig. 9 shows that the June 1969 lava flow from Pacaya's active vent is coincident with the hot thermal anomaly in Fig. 10. The sides of the lava flow radiate infrared radiation and

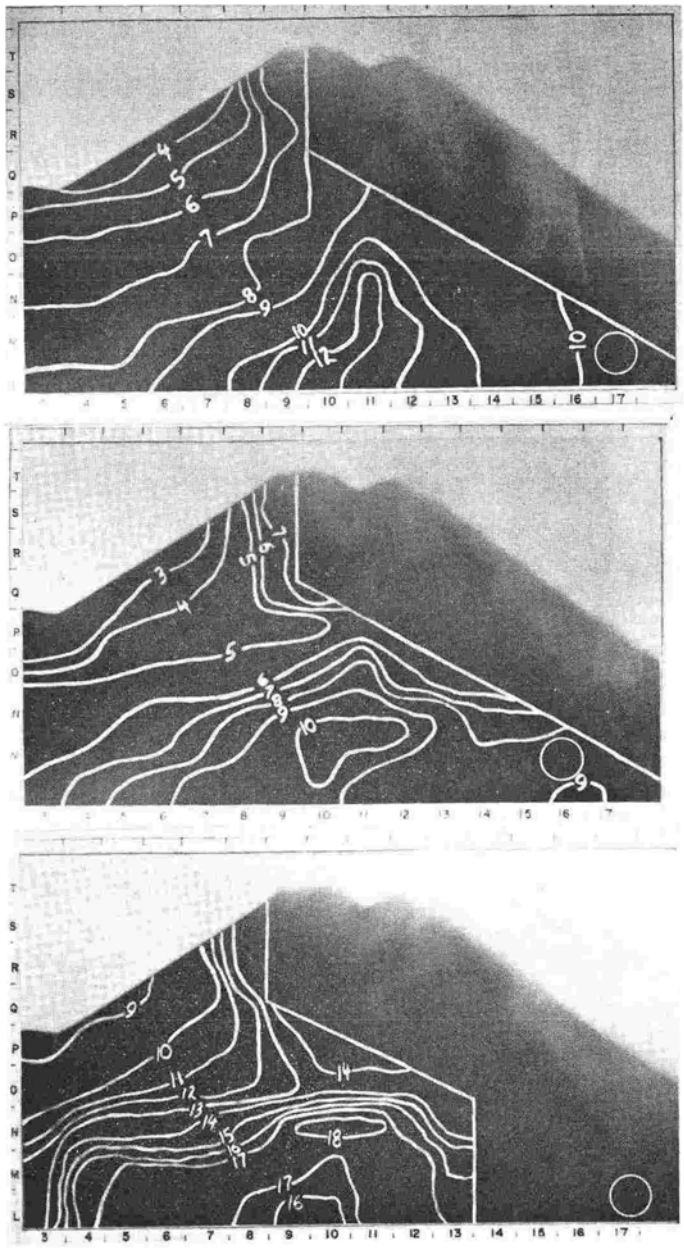

FIG. 10 - Thermal pattern of Pacaya Volcano looking southeast from Cerro Chino, 23 December 1969 (top), 30 December 1969 (middle), and 31 March 1970 (bottom). Contours indicate apparent surface temperatures in °C Grids enclose surfaces 30 ± 15 m across slope and 60 ± 20 m up slope. Eruptive activity at S-12 prevented thermal mapping of right side of cone. Circle at lower right represents 2° field of view of radiation thermometer.

the radiation strikes the lava surfaces not underlain by the lava flow. For this reason, the anomalously hot area extends beyond the physical confines of the lava flow.

Near the summit of Pacaya, the apparent surface temperatures are seen to increase in towards the explosive vent. This may be a surface manifestation of the hot pipe feeding the explosive vent, but is most likely due to hot pyroclastics lying on the surface near

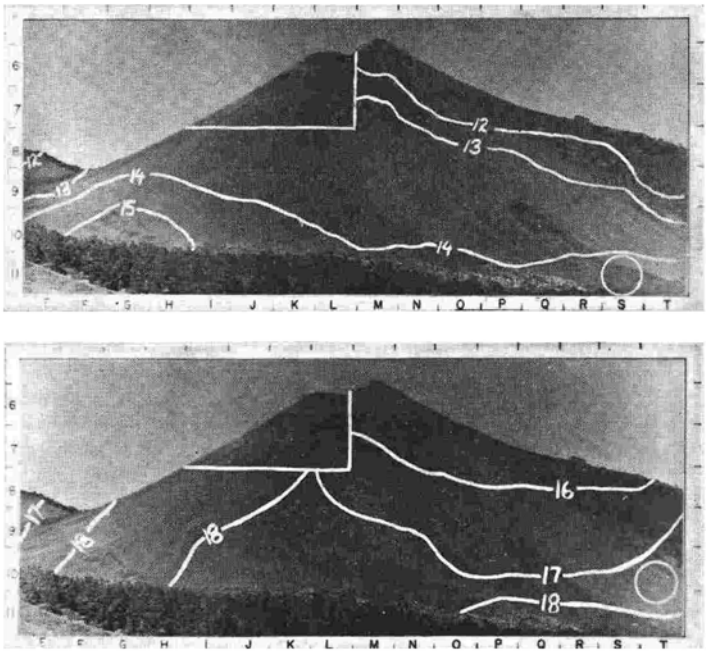

FIG. 11 - Thermal pattern of Pacaya Volcano looking northeast from Finca El Chupadero, 28 December 1969 (top) and 1 April 1970 (bottom). Cerro Chino station is just off left side of photo on ridge. Contours indicate apparent surface temperatures in °C. Grids enclose surfaces 120 ± 30 m across slope and 230 ± 50 m up slope. Eruptive activity at 6-L prevented thermal mapping of upper left portion of the volcano. Circle at lower right represents 2° field of view of radiation thermometer.

the vent. On the far left of Fig. 10, the isotherms are seen to be approximately horizontal. This area is far enough away from the lava flow so that the cooling of the surface with altitude is due to the adiabatic cooling of the atmosphere.

Apparent surface temperatures on the southwest flanks of Pacaya Volcano were mapped from a station on open land near Finca El

Chupadero along the dirt road between the villages of Dolores and El Patrocinio (Fig. 8) on the early mornings of 28 December 1969 and 1 April 1970 (Fig. 11). About 750 m of relief are present in these plates. The area sectioned off on the upper slope of Pacaya was covered with hot pyroclastics. Pyroclastics were constantly rolling down the left slope on both occasions. These pyroclastics account for the slight warming trend on the left side of Fig. 11. The right side of the thermal pattterns show a cooling with altitude observed in the preceeding thermal patterns. There is no surface manifestation of an underlying geothermal anomaly on the southwest flank of the Pacaya cone (Fig. 11).

Atmospheric Corrections

The thermal patterns discussed above were based on apparent surface temperatures. Apparent surface temperatures differ from real surface temperatures in that apparent surface temperatures are calculated assuming that the surface material has unit emissivity and that there is no absorption or emission of radiant energy in the atmospheric path between the surface and the sensor. These two assumptions do not hold for the real environment. This section will consider the effects of the atmosphere in modifying real surface temperatures.

The intensity of the infrared radiation arriving at the sensor differs from the intensity of the infrared radiation very near the surface due to attenuation and emission of radiation by the atmosphere (SAUNDERS, 1967, p. 4110). If the atmosphere partially absorbs radiation at a particular wavelength, it emits radiation at this same wavelength. The atmospheric path behaves according to the following equation:

$$\varepsilon_\lambda = \alpha\lambda = 1 - T_\lambda$$

where ε_λ, α_λ, and T_λ are the emissivity, absorptance, and fractional transmission, respectively, of the atmosperic path at wavelength λ (YATES, 1958, p. 3). If the atmosphere has a fractional transmission of 0.3, the sensor will receive 30 % of the radiation emitted by the surface and 70 % of the radiation that would be emitted by a blackbody at the temperature of the atmospheric path (YATES, 1958, p. 4).

The absorption of infrared radiation by the atmosphere depends primarily on the amount of precipitable water in the atmospheric path. The amount of precipitable water is « the thickness of the layer of liquid water which can be precipitated from the absorbing

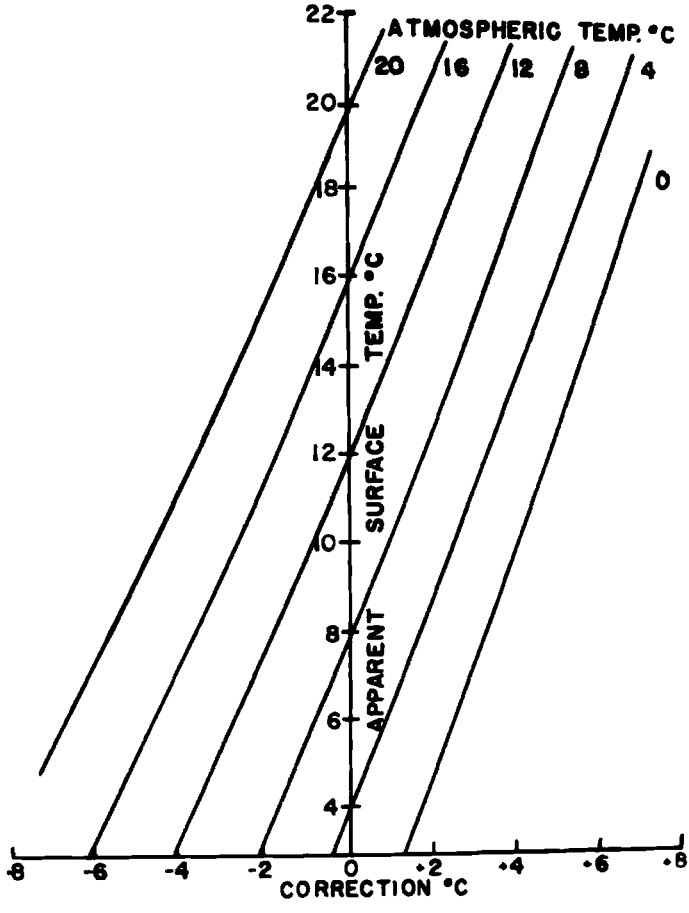

FIG. 12 - Correction factors that must be added to apparent surface temperatures for different atmospheric temperatures.

air column » (GEBBIE, *et al.*, 1951, p. 87). The atmospheric transmission of radiation in the 8-14 μ band over a path one sea mile long (1852 m) with 17 m precipitable water has been plotted by GEBBIE *et al.* (1951, p. 87). Planimetric integration of this curve shows the average transmission of the atmosphere in the 8-14 μ band to be

60 %. YATES (1958, fig. 1B) has plotted atmospheric transmission, against wavelenght over a 1000 ft (305 m) path with 2.2 mm precipitable water. Planimetric integration of Yates' curve indicates the atmospheric transmission to be 84 %. There are no data on the amount of precipitable water in the air around the volcanoes that were studied. For the sake of the following calculations, the atmospheric transmission will be assumed to have been intermediate between the above two extremes at 70 %, with a maximum variation of $\pm$ 14 %.

The actual radiant exitance originating at a surface, assuming an atmospheric transmission of 70 %, can be calculated according to the following equation:

$$W_s = (W_r - 0.30\, W_a) / 0.70$$

where W_s, W_a, and W_r are the radiant exitance originating at the surface, the radiant exitance originating in the atmosphere, and the irradiance at the sensor, respectively. The radiant exitances can be converted into apparent temperatures according to the Stefan-Boltzmann Law. Figure 12 shows graphically the correction factor that must be added to the apparent surface temperatures (based or irradiance at the sensor) for different atmospheric and apparent surface temperatures. Each of the thermal patterns that will be used in the excess radiant heat calculations in the next section are corrected for atmospheric absorption and emission of 8-14 μ radiation.

TABLE 1 - Rates of Surface Cooling With Altitude.

Thermal Pattern	*Cooling Rate °C/100 m*
Pacaya from Cerro Chino 12-23-69	1.4
Pacaya from Cerro Chino 12-30-69	1.4
Pacaya from El Chupadero 12-28-69	1.0
Pacaya from El Chupadero 4-1-70	1.3
Izalco from Cerro Verde 12-26-69	0.4
Izalco from Cerro Verde 4-3-70	0.4
Izalco from Lava Nueva 4-5-70	0.9
San Miguel from La Placita 4-4-70	0.4
Average	0.9

Air temperatures for the December 1969 patterns were recorded at the sensor stations at the time the patterns were obtained. For the March and April 1970 thermal patterns, air temperatures were not recorded. When air temperatures were not recorded, the air temperatures were estimated on the basis of regional meteorological data of the Observatorio Nacional del Servicio Meteorologico de Guatemala (VASSEAU, 1967). Air temperatures are assumed to be constant

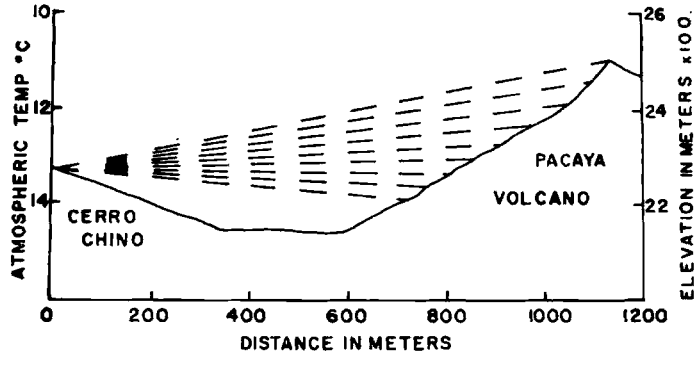

FIG. 13 - Northwest-southeast cross section through Pacaya Volcano and Cerro Chino showing the cones of the 2° field of view of the radiation thermometer and the variation of atmospheric temperature with altitude.

for constant elevations and to cool with altitude according to the dry adiabatic lapse rate of 1°C/100 m (WILLETT and SANDERS, 1959, p. 22). Based on the air temperature at the elevation of the sensor and the adiabatic lapse rate, air temperatures for all the elevations were calculated. The air temperature of an atmospheric path is taken as the average of the air temperature just above the surface of the volcano for the particular field of view being considered and the air temperature at the sensor station. An example of an atmospheric thermal profile is seen in Fig. 13. These air path temperatures are considered accurate within 2°C.

The nocturnal accumulation of cold air on poorly drained surfaces may be a problem in infrared thermal sensing (WOLFE, 1968, p. 19). Cold air is apt to fill a topographic depression and provide anomalously low atmospheric temperatures. However, it is felt that the volcanic slopes observed in this study are uniformly well drained so that no local accumulations of cold air were encountered.

The radiant exitance at the surface of the volcano was calculated according to the equation for the atmospheric absorption correction shown earlier. The radiant exitance at the surface was then converted to apparent surface temperature according to the Stefan-Boltzmann Law. These were apparent surface temperatures corrected only for atmospheric absorption, not surface emissivity. The atmospheric corrected apparent surface temperatures are those that would have been measured if the radiation thermometer had been just above the surface of the volcano, not at a remote station.

Excess Radiant Heat Calculations

It is possible to calculate the differential radiant heat emission between two portions of a thermal pattern, when both portions are radiating heat to a common third surface such as the sky. This was done for selected areas of five thermal patterns: Pacaya from Cerro Chino, 12-23-69 (Fig. 10); Pacaya from Cerro Chino, 12-30-69 (Fig. 10); El Brujo from La Isla, 12-21-69 (Fig. 6); El Brujo from La Isla, 3-27-70 (Fig. 6); and El Brujo from La Loma, 3-29-70 (Fig. 7). The area chosen for the differential radiant heat calculation at Pacaya was free of recent hot eruptive products and included the June 1969 lava flow (the area bounded by and including grid row P and grid column 13). At El Brujo, the selected area covered the upper part of the dome and avoided the lower thick talus blanket (the area bounded by and including grid row 9 and above).

Temperatures that represent an average of the coolest apparent surface temperatures in the selcted areas of each of the five thermal patterns were noted. These temperatures, corrected for atmospheric absorption, serve as a cold base and represent the temperatures of the nonanomalously hot areas. On the two Pacaya thermal patterns, the cold base is located in the upper left portion of the selected area. On the El Brujo patterns, the cold base is across the bottom of the selected area. The cold base temperatures are considered accurate within 0.5°C.

It was noted that atmospheric temperatures cool with altitude. This cooling of the atmosphere with altitude will tend to cool terrain surfaces as they increase in altitude. The surficial cooling rates over nongeothermally active areas were measured at four different times on Pacaya and four different times on the El Salvadorian volcanoes

Izalco and San Miguel. The individual cooling rates are listed in Table 1; their average rate is 0.9°C/100 m with a maximum variation of 0.5°C/100 m. This average cooling rate is slightly less than the dry adiabatic cooling rate of the atmosphere of 1°C/100 m (WILLETT and SANDERS, 1959, p. 22). The cooling of the terrain surface brought about by the cooling of the atmosphere with altitude lessens the radiative transfer of geothermal heat from the surface to the atmosphere.

This adiabatic correction factor of 0.9°C/100 m is added to the thermal patterns to counteract the effect of the adiabatic cooling of the atmosphere. This correction normalizes all apparent surface temperatures to the same base altitude and permits comparison of the radiant heat exitance at one elevation with that at another elevation.

On Pacaya, where the cold base is at the upper part of the selected area, the adiabatic correction factor is added to the underlying grid rows of thermal data (Table 2). No correction is made to the top row; the correction factor is added to the next row under; twice the correction factor is added to the next row under, etc. At El Brujo, the cold base is at the bottom of the selected area of the thermal pattern. In the case of the three El Brujo patterns, the correction factor is added in increasing increments to the overlying grid rows of thermal data (Table 2).

TABLE 2 - Calculation of Differential Radiant Heat Exitance.

$$w = (\sigma/n) \sum_{i} (T_i^4 - T_o^4)$$

w = differential radiant heat exitance, cal/cm²/sec
σ = Stefan-Boltzmann Constant = 1.354×10^{-12} cal/cm²/°K⁴/sec
n = number of thermal data points
T_i = apparent surface temperature corrected for adiabatic cooling at each thermal data point, °K
T_o = coldbase apparent surface temperature corrected for adiabatic cooling, °K

Thermal Pattern	A *	n	T_o	w
El Brujo from La Isla 12-21-69	0.2	66	381.0	4.2×10^{-4}
El Brujo from La Isla 3-27-70	0.2	66	282.1	3.9×10^{-4}
El Brujo from La Loma 3-29-70	0.3	61	286.5	5.8×10^{-4}
Pacaya from Cerro Chino 12-23-69	−0.3	55	275.8	3.6×10^{-4}
Pacaya from Cerro Chino 12-30-69	−0.4	44	274.7	2.3×10^{-4}

* A = adiabatic correction factor, °K per grid row.

The differential radiant heat exitance from the selected area of each thermal pattern is calculated according to the equation in Table 2. The radiant heat exitance at the cold base of each thermal pattern is subtracted from that of each thermal data point in the same pattern. The difference in radiant heat exitance between the cold base and each point is averaged over the selected area. The resulting differential radiant heat exitance figures for each of the five selected thermal patterns are listed in Table 2. The temperatures on which the differential radiant heat exitance calculations are based are apparent temperatures, not corrected for surface emissivity. Since these calculations depend only on radiant heat exitance at the surface, there is no need to include the surface emissivities in the calculations. The surface emissivity was erroneously included in the calculations of DECKER and PECK (1967) but accounted for only a 5 % error in their final figures. It should be pointed out that the apparent surface temperatures are based on radiant exitance only in 8-14 μ spectral band. The radiant heat exitance over the whole spectrum is then calculated by using these temperatures in the Stephan-Boltzmann Law. Therefore, it is assumed the spectral emissivity of the surface materials over the whole spectrum is the same as that of the 8-14 μ spectral band. Clearly, this is not true. However, due to the unavailability of extensive emissivity data and for the sake of comparing this data with data calculated on the basis of similar assumptions, this study will maintain the assumption that the surface emissivities are constant over the whole spectrum.

The differential radiant heat exitance is the radiant heat exitance greater than that of the background nongeothermally active areas. It is, therefore, the excess radiant heat exitance caused by an anomalous geothermal feature such as a near surface magma chamber or a lava flow. Henceforth in this paper, the differential radiant heat exitance (quantity w in Table 2) will be referred to as the excess radiant heat.

The excess radiant heat figures for Pacaya and El Brujo are accurate within 61 % and 40 %, respectively. The overall error is arrived at by taking the square root of the sum of the squares of the percentage error contributions of the individual variables involved in the excess radiant heat calculation: adiabatic cooling correction factor, atmospheric absorption, atmospheric path temperature, cold base temperature, and apparent surface temperature. The Pacaya error is greater than the El Brujo error because the difference

between the atmospheric path temperatures and apparent surface temperatures at Pacaya are greater than those of El Brujo. All five excess radiant heat figures are within an order of magnitude of the 9.57×10^{-4} cal/cm^2/sec figure obtained by DECKER and PECK (1967, p. D173) for the excess radiant heat at Alae Lava Lake, Hawaii between 5 : 10 and 5 : 30 A.M.

DECKER and PECK (1967) also calculated the total heat flow from Alae Lava Lake, Hawaii. Total heat flow is obtained by multiplying the thermal conductivity of the lava by the geothermal gradient. It was observed that the excess heat loss by surface radiation in the early morning represented about 20 % of the total heat flow from the cooling lava lake. DECKER and PECK (1967, p. D175) speculate that the rest of the heat was lost by « evaporation of rain, transfer by escaping gases, and conduction and convection of the contact air layer ».

The average of the 12-23-69 and 12-30-69 excess radiation heat figures at Pacaya is 3.0×10^{-4} cal/cm^2/sec. If 20 % of the total heat flow at Pacaya in the early morning is accounted for by excess radiant heat emission, as was the case at Alae Lava Lake, Hawaii, then the total heat flow at Pacaya was 1.5×10^{-3} cal/cm^2/sec. The figure is three orders of magnitude greater than the average heat flow from the surface of the earth which is approximately 1.4×10^{-6} cal/cm^2/sec (LEE, 1965, p. 35).

The recent eruptive products at Pacaya are basalts (EGGERS, 1972). Since the thermal conductivity of the basalt is known [3.4×10^{-3} cal/cm/sec/°C (DECKER and PECK, 1967)], the geothermal gradient is calculated according to the standard heat flow equation to be 0.4°C/cm. By taking the geothermal gradient to be 0.4°C/cm, the melting temperature of basaltic lava to be 1050°C (YODER and TILLEY, 1962, p. 463), and the lava surface temperature to be 15°C, the depth to molten lava is calculated to be 26 m. Carrying on the 61 % error in the excess radiant heat calculations at Pacaya, the geothermal gradient is accurate between 0.2 and 0.7°C/cm and the depth to molten lava is accurate between 15 and 51 m.

The excess radiant heat at Pacaya is due to the buried June 1969 lava flow. The lava flow was no greater than 5 m thick at the time of emplacement (EGGERS, personal communication, September 1970). Taking this thickness as a maximum, it is possible to calculate according to the model of JAEGER (1961, p. 730) that the portion of the lava flow included within the thermal pattern had completely

solidified within 59 days after emplacement (Table 3). Jaeger's model is based only on cooling by conduction and must be taken as a maximum time. If convective or radiative cooling were taken into account, the cooling rate would be faster. Therefore, it is clear that the June 1969 flow was completely solidified in December 1969 when the initial radiation data were taken. The radiation data taken in December 1969 also indicate that the lava flow had completely solidified, for the calculated geothermal gradient requires a thickness, greater than the thickness of the lava flow to reach melting temperatures. The depth required for melting temperatures is 26 m while the thickness of the lava was no greater than 5 m.

TABLE 3 - Calculation of Cooling Time for June 1969. Lava Flow at Pacaya

$\tau = kt/d^2$ (after LOVERING, 1935; and JAEGER, 1961, p. 722)

τ = dimensionless term proportional to time of emplacement of lava flow and relates extrusive lava sheets of all thicknesses to the same set of curves = 0.14 [see footnote (1) below]

k = thermal diffisivity = 6.8×10^{-3} cm²/sec (BIRCH, 1942, p. 253)

t = time after emplacement, sec

d = thickness of extrusive sheet = 500 cm [maximum estimate after EGGERS (personal communication, September 1970)]

$t = \tau d^2/k = 5.1 \times 10^6$ sec = 59 days (time for lava to solidify)

(1) Calculation of τ:

T_o = temperature of lava at time of emplacement = 1250°C [maximum temperature of basaltic lava observed on surface (LEE and CLARK, 1966, p. 511)]

T = temperature of lava at solidification = 1050°C (YODER and TILLEY, 1962, p. 463)

$T/T_o = 0.8$ at the moment of solidification according to JAEGER (1961, p. 730, fig. 11), if $T/T_o = 0.8$ then the maximum possible value for τ will be 0.14.

The three values of excess radiant heat from the El Brujo Dome are in close agreement (Table 2). The average of these three values is 4.6×10^{-4} cal/cm²/sec. If this figure represents 20 % of the total early morning heat flow, as was observed by DECKER and PECK (1967, p. D174) at Alae Lava Lake, Hawaii, the total heat flow from El Brujo Dome is 2.3×10^{-3} cal/cm²/sec. This figure is assumed to apply to the whole dome, but represents observations from two angles that cover about one half of the dome. The El Brujo heat flow figure

is the same order of magnitude as that observed at Pacaya and also three orders of magnitude greater than the world average. The Santiaguito rocks are hornblende hypersthene andesite (STOIBER and ROSE, 1969, p. 481). Based on the thermal conductivity of andesite [3.06×10^{-3} cal/cm/sec/°C (BIRCH, 1942, p. 252)], the geothermal gradient on El Brujo Dome is calculated to be 0.8°C/cm. Using 875°C as the temperature change from ambiant to liquid andesite (ROSE, 1970, p. 22) and a geothermal gradient of 0.8°C/cm, the depth to molten rock at El Brujo Dome is calculated to be 11 m. By taking the error in excess radiant heat flow at El Brujo to be 40 %, the geothermal gradient is accurate between 1.0 and 0.5°C/cm and the depth to molten lava is accurate between 9 m and 19 m. On the basis of extensive field observations on and around the El Brujo Dome, Richard Stoiber and William Rose, Jr. (personal communication, August 1970) estimate the thickness of the crust over the magma chamber to be between 5 and 10 m. These figures are also in close agreement with the 5-15 m estimate for the thickness of the crust of the Merapi Lava Dome, Indonesia (VAN BEMMELEN, 1949, p. 198, footnote 1).

These calculations are based on the fact that the excess heat radiated from Alae Lava Lake in Hawaii in the early morning represented 20 % of the total conducted heat flow to the surface (DECKER and PECK, 1967). The radiant exitance is a function of the surface temperature and surface emissivity. The surface emissivity, a constant, will be discussed in the next section. The surface temperatures may vary considerably with the near surface micrometeorological conditions. However, all surface temperatures within a given thermal pattern are expected to vary in a similar manner under a particular set of micrometeorological conditions. Therefore, the temperature and radiant exitance difference between each thermal data point and the cold base is expected to be constant, regardless of the microclimate. The constancy permits the extrapolation of the 20 % ratio of excess radiant heat to conducted heat and allows the calculation of the geothermal gradient.

In extensively fissured areas, convective transfer of heat through fumaroles may effect the radiation to conduction ratios. However, there was very little fumarolic activity in the selected areas of the Santiaguito and Pacaya thermal patterns. ROBERTSON and DAWSON (1964) have noted at Wairakei thermal field, New Zealand that the dominant mechanism for heat transfer through the ground is conduc-

tion until the thermal gradients exceed 0.25°C/cm. At gradients greater than this, heat transfer by means of convection of air and water vapor become more important (ROBERTSON and DAWSON, 1964, p. 142). This author observed gradients of 0.4°C/cm and 0.8°C/cm at Pacaya and Santiaguito, respectively. Though these gradients are greater than 0.25°C/cm, it should be noted that the conductivity of the Pacaya and Santiaguito rocks is an order of magnitude greater than the 4×10^{-4} cal/sec/cm/°C conductivity of the pumice soil at Wairakei (DAWSON and FISHER, 1964, p. 153). The greater thermal conductivity in the selected areas, indicates that conduction is still the dominant heat transfer mechanism for the areas in this study, even at gradients slightly above 0.25°C/cm.

The extrapolation of Decker and Peck's (1967) excess radiant heat data to other areas to predict a geothermal gradient implies that the size of the areas over which the radiant heat data were collected are the same. Decker and Peck's (1967) hot base stations were located every foot along a profile 102 feet long which was considered representative of the central portion of the lava lake whose diameter is between 800 and 1000 feet. The areas studied in this report were between 600 and 1100 feet on a side. It is concluded that the scale of the feature studied by Decker and Peck is approximately equivalent to the scales of the features in this study.

Emissivity Corrections

According to Kirchoff's Law, the spectral radiant exitance from a real body (W_λ) equals the product of its spectral emissivity (ε^λ) and the spectral radiant exitance of a blackbody ($W_{\lambda b}$) at the same temperature: $W_\lambda = \varepsilon_\lambda \; W_{\lambda b}$ (SIMON, 1966, p. 13). The apparent temperatures discussed previously were not corrected for surface emissivity. Since real body emissivities are less than one, the apparent surface temperatures must be corrected upward to represent the real surface temperatures.

DANIELS (1966 and 1967) has measured the spectral emissivity of natural rock surfaces in the 8-14 μ band. DANIELS (1967, p. 7) gives the emissivity of a banded andesite with feldspar phenocrysts from a lava dome to be 0.90. This rock is considered close to that of the Santiaguito lava dome. DANIELS (1967, p. 7) gives the emissivity of a black, vesicular basalt as 0.91. This rock is considered close to

the vesicular olivine basalt of Pacaya Volcano. Since the emissivities of a pumiceous rhyolite and a welded portion of the Bishop Tuff are both reported as 0.91 (DANIELS, 1967, p. 5-6), it appears that the chemical composition of the extrusive volcanic rocks doesn't affect the surface emissivity by greater than 0.01. This close agreement gives confidence to the values chosen for the respective volcanoes.

The Stefan-Boltzmann Law states that the radiant exitance of a real body (W) equals the product of its real temperature in degrees Kelvin (T_r) to the fourth power, the Stephen-Boltzmann Constant (σ), and its emissivity (ε):

$$W = \sigma \varepsilon T_r^4$$

Given the apparent temperatures and the emissivity of a surface, it is possible to calculate its real body temperature on the basis of the following equation:

$$T_r = (T_a^4/\varepsilon)^{1/4}$$

where T_r and T_a are the real body temperature and apparent temperatures, respectively, and ε is the emissivity of the real body.

Assuming that all rocks at Santiaguito have 0.90 emissivity, a correction of between 7° and 8°C should be added to all apparent temperatures to get real surface temperatures. Assuming that the emissivity of all Pacaya is 0.91, a correction factor of between 6.5 and 7.5°C should be added to the apparent surface temperatures to get real body surface temperatures. The variation of apparent and real temperatures for different emissivities is shown graphically in Fig. 14.

By combining the emissivity and the atmospheric corrections with the apparent surface temperatures, one arrives at the real surface temperatures. This is the temperature that would be measured directly on the surface of the rock. A comparison of apparent surface temperatures and real surface temperatures is given diagrammatically in Fig. 15. The general shape of the thermal patterns remain the same, though the real surface temperatures are about 5°C warmer than the apparent surface temperatures. Figure 15 also shows the thermal pattern of surface temperatures associated with the excess radiant heat. These temperatures are apparent surface temperatures corrected for atmospheric absorption and adiabatic cooling of the

atmosphere and minus the cold base surface temperature. These temperatures can be converted to radiant heat by the Stefan-Boltzmann Law. It can be seen that the horizontal isotherms associated

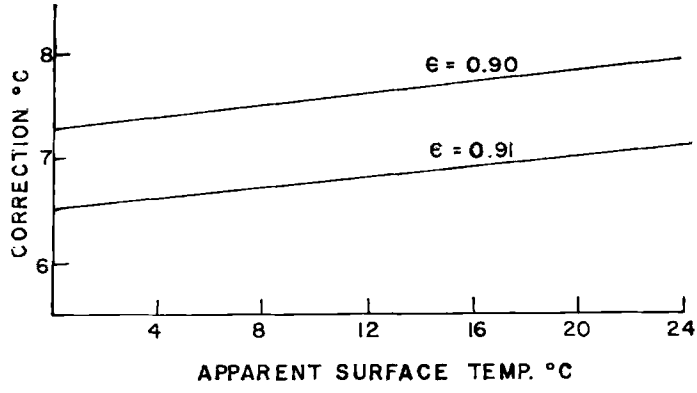

FIG. 14 - Correction factors for surface emissivity that must be added to apparent surface temperatures (corrected for atmospheric absorption) to get real surface temperature.

with the cooling atmosphere with altitude on the left of the uncorrected thermal pattern have disappeared though the contours associated with the June 1969 lava flow are still present.

Predicted Effects of Magma Movement

The geothermal gradient underlying El Brujo Dome has been shown to be 0.8°C/cm. Therefore, the solidus interface of andesite is reached at 11 m depth. It now remains to investigate the effects of an instantaneous upward movement of magma from 11 m to 5.5 m depth. The temperature change between liquid and ambiant andesite is assumed to remain unchanged at 875°C.

The upward movement of magma will double the geothermal gradient to 1.6°C/cm and double the total heat flow to the surface to 4.6×10^{-3} cal/cm^2/sec. It is anticipated that the thermal effects of this upward movement of magma would be seen almost immediately in fumaroles and fissures on the surface due to the rapid upward convection of heat. However, if the heat were allowed to

make its way to the surface only by the mechanism of conduction through the solid rock, the thermal effects would be seen on the surface much later.

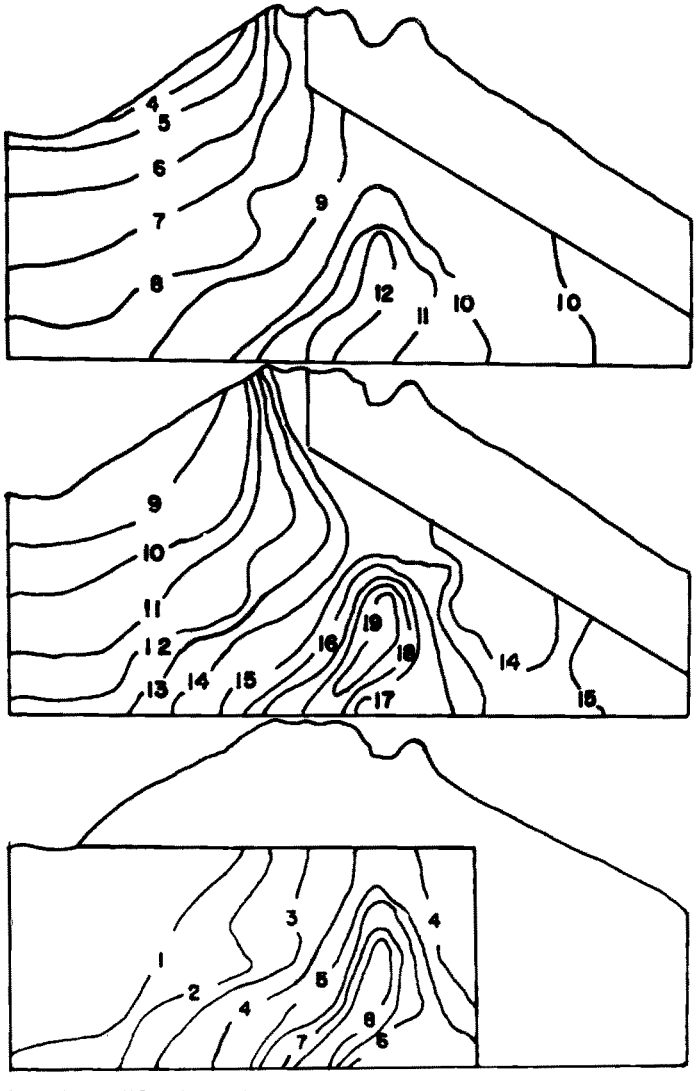

FIG. 15 - Selected modification of the 23 December 1969 thermal pattern of Pacaya Volcano as seen from Cerro Chino. Top: apparent surface temperatures in °C. Middle: real surface temperatures with corrections made for atmospheric absorption and surface emissivity. Bottom: excess radiant heat pattern of apparent surface temperatures corrected for atmospheric absorption and cooling minus the cold base.

The effects of the magma movement on the geothermal gradient can be seen in the equation of CALRSLAW and JAEGER (1959, p. 100):

$$V = V_2(X/d) + (2/\pi) \sum_{n=1}^{\infty} \frac{V_2 \cos(n\pi)}{n} \sin(n\pi X/d) \exp(-kn^2\pi t/d^2)$$

where V is the temperature (°C) at depth X (cm), d is the thickness of rock (cm) separating the surface and the magma, V_2 is the tem-

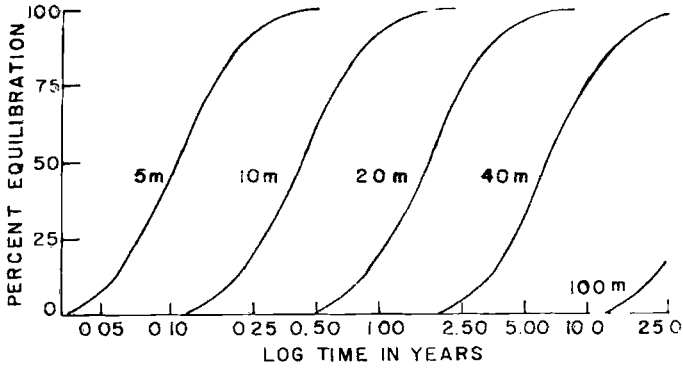

FIG. 16 - Percent equilibration of the geothermal gradient at the surface for different crustal thicknesses.

perature difference (°C) between liquid and ambiant andesite, k is the thermal diffusivity of the rock (cm²/sec), and t is the time (sec). For these calculations, the surface is assumed to be at 0°C, and the thermal diffusivity for andesite is taken as 1.24×10^{-2} cm²/sec (BIRCH, 1942, p. 292) and considered independent of temperature. By taking the derivative of the above equation with respect to X, the geothermal gradient at the surface ($X = 0$) is seen to vary over time according to the following equation:

$$\frac{dV}{dX} = \frac{V_2}{d}[1 - 2\exp(-k\pi^2 t/d^2) + 2\exp(-4k\pi^2 t/d^2) - 2\exp(-9k\pi^2 t/d^2)\ldots].$$

Considering the case of the 5.5 m crustal thickness of El Brujo Dome, the percent equilibration of the geothermal gradient indicates that the surface shows no effects of the subsurface magma movement until twelve days after the upsurgence. It takes over four months for gradient to fully equilibrate. Twelve days is taken as the minimum time for the surface to thermally manifest the subsurface magma movement and as the minimum time required for the magma movement to be monitored by infrared radiation thermometry.

Figure 16 shows the percent equilibration of the geothermal gradient for different crustal thicknesses plotted against the log of time and using an average diffusivity of 0.01 cm^2/sec. There is an exponential increase in time with increase in crustal thickness for the surface to register changes in its geothermal gradient following a subsurface magma movement.

Unless one is dealing with a very shallow magma chamber or unless there is a transfer of heat to the surface by mechanisms other than pure conduction through the rock, it appears that considerable periods of time are required for the thermal effects of a subsurface magma movement to be thermally manifested on the surface.

Summary and Conclusions

This study has proved the feasibility and rapidity of a land-based remote infrared radiation thermometry survey to obtain information on the geothermal state of a volcano. A Barnes PRT-5 precision radiation thermometer is used to obtain eleven thermal patterns of six different volcanic surfaces from land-based stations. A time interval of three months separated four of the thermal patterns and permitted observation of time related changes in the thermal regime of the volcanoes under study.

The thermal data are corrected for the effects of atmospheric absorption of infrared radiation, surface emissivity, and the adiabatic cooling of the atmosphere with altitude. The thermal patterns delineate areas of fumarolic activity and active domal upgrowth. At Pacaya Volcano the nongeothermally active areas cool with altitude due to the adiabatic cooling of the atmosphere with altitude. At El Brujo, however, apparent surface temperatures increase with altitude due to the thinning of the insulating talus blanket with altitude.

Based on excess radiant heat calculations, it is concluded that the June 1969 lava flow from Pacaya Volcano had completely solidified by December 1969. This conclusion is consistent with theoretical calculations on the cooling of an extrusive lava sheet by conduction.

Excess radiant heat calculations indicate that the magma chamber underlying the El Brujo Dome, a unit of the Santiaguito Volcanic Dome, is at a depth of 11 m with maximum variation of between 9 m and 19 m. This figure is consistent with field observations in the area.

The four thermal patterns that were mapped in December 1969 and again in March 1970 show a very similar pattern of isotherms whose absolute temperature variations resulted from different atmospheric temperatures. There is a high degree of repeatability in these infrared measurements. The repeatability is imperative if one is to undertake a series of observations spread out over time.

Provided that magma movements toward the surface are slower than the times required for their thermal effects to be manifested at the surface, infrared thermal patterns spread out over time would provide a means of monitoring changes in an underground magma reservoir and of predicting impending volcanic activity.

Acknowledgements

This study was financed in part by the U.S. Army Cold Regions Research and Engineering Laboratory (USA CRREL), Hanover, N. H., and the National Science Foundation (Grant No. GA 1533). The author is indebted to Dr. Richard Stoiber, Professor of Geology at Dartmouth College, Hanover, N. H., for his tireless assistance in all aspects of the study. Help was received from the staff of the Photographic Interpretation Research Division of USA CRREL, in particular, Mr. Robert Frost, Chief of the Division, who provided the infrared radiation thermometer, and Mr. Ambrose Poulin, Research Civil Engineer. Dr. Francis Birch, Professor of Geophysics at Harvard University, aided the author in interpreting the heat flow equations.

Assistance in the field was provided by Dr. Ian Lange, Mark Nibbelink and John Valley. Mr. Oscar Salazar of the Institute Geográfico Nacional, Guatemala, and Dr. Henry Meyer of the United Nations Projecto Minero, El Salvador, provided vehicular support for the author while in the field.

References

BARNES ENGINEERING Co., 1968, *Instruction Manual for Precision Radiation Thermometer Model PRT-5;* Barnes Engineering Co., 30 Commerce Rd., Stamford, Conn.

BIRCH, F., 1942, *Thermal conductivity and diffusivity.* In *Handbook of Physical Constants,* ed. by BIRCH, F., *Schairer,* J. F., and SPICER, H. C., Geol. Soc. Am. Spec. Paper No. 36, p. 243-266.

CARLSLAW, H. S. and JAEGER, J. C., 1959, *Conduction of Heat in Solids,* 2nd ed. Oxford University Press, Great Britain, 510 pp.

DANIELS, D. L., 1966, *Infrared spectral emittance of rocks from the Pisgah Crater and Mono Craters Areas, California.* N.A.S.A., Tech. Letter NASA-13.

————, 1967, *Additional Infrared Spectral Emittance Measurements of Rocks from the Mono Craters Region, California.* Prepared by U.S.G.S. for N.A.S.A., Interagency Rept. NASA-90.

DAWSON, G. B. and FISHER, R. G., 1964, *Diurnal and seasonal ground temperature variations at Wairakei.* New Zealand Journ. Geol. and Geophys., 7, p. 144-154.

DECKER, R. W. and PECK, D. L., 1967, *Infrared radiation from Alae Lava Lake, Hawaii.* U.S.G.S. Prof. Paper 575-D, p. D169-D175.

EGGERS, A. A., 1972, *The geology and petrology of the Amatitlán quadrangle, Guatemala.* Ph. D. Thesis, Dartmouth College, Hanover, N.H.

FISCHER, W. A., MOXHAM, R. M., POLCYN, F., and LANDIS, G. H., 1964, *Infrared studies of Hawaiian volcanoes.* Science, *146,* no. 3645, p. 733-742.

FRIEDMAN, J. D. and WILLIAMS, R. S., Jr., 1968, *Infrared sensing of active geologic processes.* Proc. Fifth Symp. on Remote Sensing of Environment, Univ. of Michigan Inst. of Sci. and Tech., Ann Arbor, Mich., p. 787-820.

GEBBIE, H. A., HARDING, W. R., HILSUM, C., PRYCE, A. W., and ROBERTS, V., 1951, *Atmospheric transmission in the 1-14 μ region.* Proc. Roy. Soc. of London, Series A, Mathematical and Physical Sciences, *206,* p. 87-107.

HERSCHEL, J. F. W., 1840, *Account of a process of rendering visible the calorific spectrum by its effect on paper properly prepared and some further results obtained respecting the distribution of heat therein.* Trans. Roy. Soc. London, Part 1, p. 51-59.

JAEGER, J. C., 1961, *The cooling of irregularly shaped igneous bodies.* Am. Journ. Sci., *259,* p. 721-734.

LEE, W. H. K. (ed.), 1965, *Terrestrial Heat Flow.* Am. Geophys. Union Mono. *8,* 276 pp.

———— and CLARK, S. P., Jr., 1966, *Heat flow and volcanic temperature.* In *Handbook of Physical Constants,* S. P. CLARK, Jr. (ed.), G.S.A. Mem. *97,* p. 483-511.

LOVERING, T. S., 1935, *Theory of heat conduction applied to geological problems.* Geol. Soc. Am. Bull., *46,* p. 69-94.

MCLERRAN, J. H., 1967, *Infrared thermal sensing.* Photogram. Eng., *33,* no. 5, p. 507-512.

MEYER-ARNDT, J. R., 1968, *Radiometry and photometry: units and conversion factors.* Applied Optics, *7,* no. 10, p. 2081-2084.

MEYER-ABICH, H., 1958, *Active volcanoes of Guatemala and El Salvador.* In *Catalogue of the Active Volcanoes of the World Including Solfatara Fields, Part VI Central America,* by F. Mooser, H. Meyer-Abich, and A. R. McBirney, Int. Volcanological Assoc., Naples, p. 39-105.

MILLER, L. D., 1966, *Location of anomalously hot earth with infrared imagery in Yellowstone National Park.* Proc. Fourth Symp. on Remote Sensing of Environment, Univ. of Mich. Inst. of Sci. and Tech., Ann Arbor, Mich., p. 751-769.

MOOSER, F., MEYER-ABICH, H., and MCBIRNEY, A. R., 1958, *Catalogue of the Active Volcanoes of the World Including Solfatara Fields, Part VI Central America.* Int. Volcanological Assoc., Naples.

MOXHAM, R. M., 1969, *Aerial infrared surveys at the Geysers geothermal steam field, California.* U.S.G.S. Prof. Paper 650-C, p. C106-C122.

————, 1971, *Thermal features at volcanoes in the Cascade Range, as observed by aerial infrared surveys.* Bull. Volcanologique, *34*, no. 1, p. 77-106.

———— and ALCARAZ, A., 1966, *Infrared surveys at Taal Volcano, Philippines.* Proc. Fourth Symp. on Remote Sensing of Environment, Univ. of Mich. Inst. of Sci. and Tech., Ann Arbor, Mich., p. 827-843.

————, CRANDELL, D. R., and MARLATT, W., 1965, *Thermal features at Mount Rainier, Washington, as revealed by infrared surveys.* U.S.G.S. Prof. Paper 525D, p. D93-D100.

ROBERTSON, E. L. and DAWSON, G. B., 1964, *Geothermal heat flow through the soil at Wairakei.* New Zealand Journ. Geol. and Geophys., 7, p. 134-143.

ROSE, W. I., Jr., 1967, *Notes on fumaroles and recent activity of Volcan Pacaya.* In *Excursion Guidebook for Guatemala;* S. BONIS (ed.), Inst. Geografico Nacional, Guatemala, Geol. Bull. no. 4, p. 31-33.

————, 1970, *The Geology of the Santiaguito Volcanic Dome, Guatemala.* Ph. D. Thesis, Dartmouth College, Hanover, N.H.

————, 1972, *Santiaguito Volcanic Dome, Guatemala.* G.S.A. Bull., *83*, p. 1413-1434.

————, STOIBER, R. E., and BONIS, S. B., 1970, *Volcanic activity at Santiaguito Volcano, Guatemala.* Bull. Volc., *34*, no. 1, p. 295-307.

SAUNDERS, P. M., 1967, *Aerial measurements of sea surface temperature in the infrared.* Journ. Geophys. Res., 72, no. 16, p. 4109-4117.

SHILIN, B. V. and GUSEV, N. A., 1969, *Thermal aerial survey of Kamchatka volcanoes.* Sovetskaya Geologiya (Soviet Geology), *12*, no. 5, p. 139-147, trans. by L. Thompson, Foreign Technology Division, Wright-Patterson Air Force Base, Ohio.

————, GUSEV, N. A., MIROSHNIKOV, M. M., and KARIZHENSKI, YE. YA., 1969, *Infrared aerial survey of the volcanoes of Kamchatka.* Proc. Sixth Int. Symp. on Remote Sensing of Environment, Inst. of Sci. and Tech., Univ. of Mich., Ann Arbor, Mich., p. 175-187.

———— and KOMAROV, V. B., 1968, *Application of infrared aerial recording techniques to studies of volcanoes and thermal activities of Kamchatka Peninsula.* The Ministry of Geology of the U.S.S.R. The Laboratory for Aerial Techniques, Leningrad; trans. by A. Birko, Willow Run Laboratories, Institute of Sci. and Tech., Univ. of Mich., Ann Arbor, Mich. (8 pages).

SIMON, I., 1966, *Infrared Radiation.* Van Nostrand Momentum Book #12, 119 pp.

STOIBER, R. E. and ROSE, W. I., Jr., 1969, *Recent volcanic and fumarolic activity at Santiaguito Volcano, Guatemala.* Bull. Volcanologique, *33*, no. 2, p. 475-502.

VAN BEMMELEN, R. W., 1949, *The Geology of Indonesia, and Adjacent Archipelagos.* Government Printing Office, The Hague.

VASSEAU, J. P., 1967, *Principle climatological elements of the region south of Quezaltenango, Guatemala.* Unpublished data, Observatorio Nacional del Servicio Meterologico de Guatemala, Guatemala, C. A.

WILLETT, H. C. and SANDERS, F., 1959, *Descriptive Meteorology.* Academic Press, N. Y., 355 pp.

WILLIAMS, H., 1960, *Volcanic History of the Guatemalan Highlands.* Univ. of Cal. Press, Berkeley and Los Angeles.

WOLFE, E. W., 1968, *Geologic evaluation of thermal infrared imagery, Caliente and Temblar Ranges, Southern California.* Prepared by U.S.G.S. for N.A.S.A., Interagency Rept. NASA-113.

YATES, H. W., 1958, *The Influence of Atmospheric Absorption on Radiation Measurements.* Barnes Engineering Co., 30 Commerce Rd., Stamford, Conn.

YODER, H. S., Jr. and TILLEY, C. G., 1962, *Origin of basaltic magmas; an experimental study of natural and synthetic rock systems.* Journ. of Pet., *3,* no. 3, p. 342-532.

Manuscript received Sept. 1972